AIP | Review of Scientific Instruments

Meteorological radiosonde interface for atmospheric ion production rate measurements

R. G. Harrison

Citation: Rev. Sci. Instrum. **76**, 126111 (2005); doi: 10.1063/1.2149005
View online: http://dx.doi.org/10.1063/1.2149005
View Table of Contents: http://rsi.aip.org/resource/1/RSINAK/v76/i12
Published by the American Institute of Physics.

Meteorological radiosonde interface for atmospheric ion production rate measurements

R. G. Harrison[a)]
Department of Meteorology, The University of Reading, P.O. Box 243, Earley Gate, Reading, Berks RG6 6BB, United Kingdom

(Received 9 September 2005; accepted 14 November 2005; published online 27 December 2005)

A disposable balloon-carried instrument, interfaced to a commercial meteorological radiosonde for measuring the atmospheric ion production rate, is described. The sensor used is a gamma-sensitive Geiger tube, operated at 550 V bias, produced from a lightweight transformerless supply. The supply requires 15 V at 10 mA, and precision regulation is used to minimize the Geiger tube's response to bias voltage changes. The supply was stable to 0.1% for supply voltage variations between 15 and 25 V, and varied by less than 1% over temperatures from −53 to 25 °C during an atmospheric ascent. A digital counter incremented with each Geiger tube event, and the instantaneous count value was telemetered over a radiolink, time-stamped on reception to obtain the count rate. The derived ion production rate profile agrees with a standard parametrization to 5%.
 [DOI: 10.1063/1.2149005]

Charge exchange in the lower troposphere occurs through collisions between molecular ions and aerosol particles, leading to aerosol electrification.[1] Preferential removal of charged aerosol to water droplets[2,3] physically links the electrical and radiative properties of the atmosphere. As the production rate of ions is important in determining both the steady-state aerosol charge, and the rate at which the steady-state charge is achieved,[4] measurement of the ion production rate in cloud-forming regions is necessary in assessing the significance of charge-induced radiative changes on climate.[5]

Atmospheric ion production rate measurements have been obtained using balloon-borne ion chambers,[6] but generally the equipment has to be temperature stabilized and recovered after the balloon has burst. A meteorological radiosonde carrying a gamma radiation Geiger-Müller tube presents an inexpensive and physically compact alternative, and provides additional measurements from which the air density can be calculated. The relationship between Geiger tube count rate and equivalent charge production per unit mass of air is specified by the Geiger tube sensitivity S (Roentgens/h) at unit count rate (1 count s^{-1}), where one Roentgen is the quantity of x rays or γ radiation producing 2.58 mC of charge in 1 kg of air. For a Geiger tube count rate R, the ion-pair production rate q per unit volume, in air of density ρ, is

$$q = \frac{2.58 \times 10^{-9}}{3600} \frac{SR\rho}{2e}, \tag{1}$$

where e is the elementary charge (Coulombs). Units of the other quantities are q ($cm^{-3}\ s^{-1}$), ρ ($kg\ m^{-3}$), and R (counts s^{-1}).

Although radiosondes have a long history in atmospheric cosmic ray measurements,[7,8] a difficulty is the need for a lightweight and temperature-stable high tension (HT) bias supply for the Geiger tube. A Geiger tube's voltage response curve typically includes a "plateau" region, where it shows the least, but nonzero, sensitivity to bias voltage changes. For the miniature LND714 gamma detector Geiger tube,[9] the sensitivity change in the plateau region (at 450-650 V bias voltage) is 15% for a 100 V change in the bias voltage. To maintain the tube count rate sensitivity to 1% on a radiosonde, the HT bias voltage therefore needs to be stable to better than 1% in 650 V, through temperature changes of ~100 °C, and supply voltage changes from ageing of the radiosonde battery.

A precision HT supply has been developed to provide this performance, combined with a data acquisition system for the Vaisala RS80 radiosonde.[10] A LND714 Geiger tube was used as the sensor, and connected using a digital counter interface to the data acquisition system. The HT supply used a switching regulator configuration to generate up to 600 V from the nominal 18 V battery; the digital counter was 8 bits, with a serial output. By the use of miniature inductors rather than a transformer, the circuit board including the LND714 tube, HT supply, and digital interface on a fiberglass printed circuit board had a total mass of 36 g. The RS80 radiosonde provides standard meteorological measurements of air temperature, pressure, and relative humidity.

Figure 1 shows a schematic of the HT supply and digital interface circuit. It is based around a 6.7 kHz op-amp square wave oscillator (IC2a), which drives a high voltage (600 V) metal-oxide semiconductor field-effect transistor (MOSFET) Q1 in switching a load of two series-connected 4.7 mH axial inductors. The HT produced is rectified by D1, smoothed by C4, and delivered to the Geiger tube GT1 through R9. A fixed fraction of the HT (at R7-R8) is compared by IC2b against an adjustable (at VR1) reference voltage. The difference is amplified by IC2b to control the oscillator, regulating the HT voltage. IC5 protects against overvoltage damage when the wet battery of the radiosonde is freshly activated by limiting the supply to 18 V. C8 and C9 provide decoupling, preventing the oscillator from interfering with the ra-

[a)]Electronic mail: r.g.harrison@reading.ac.uk

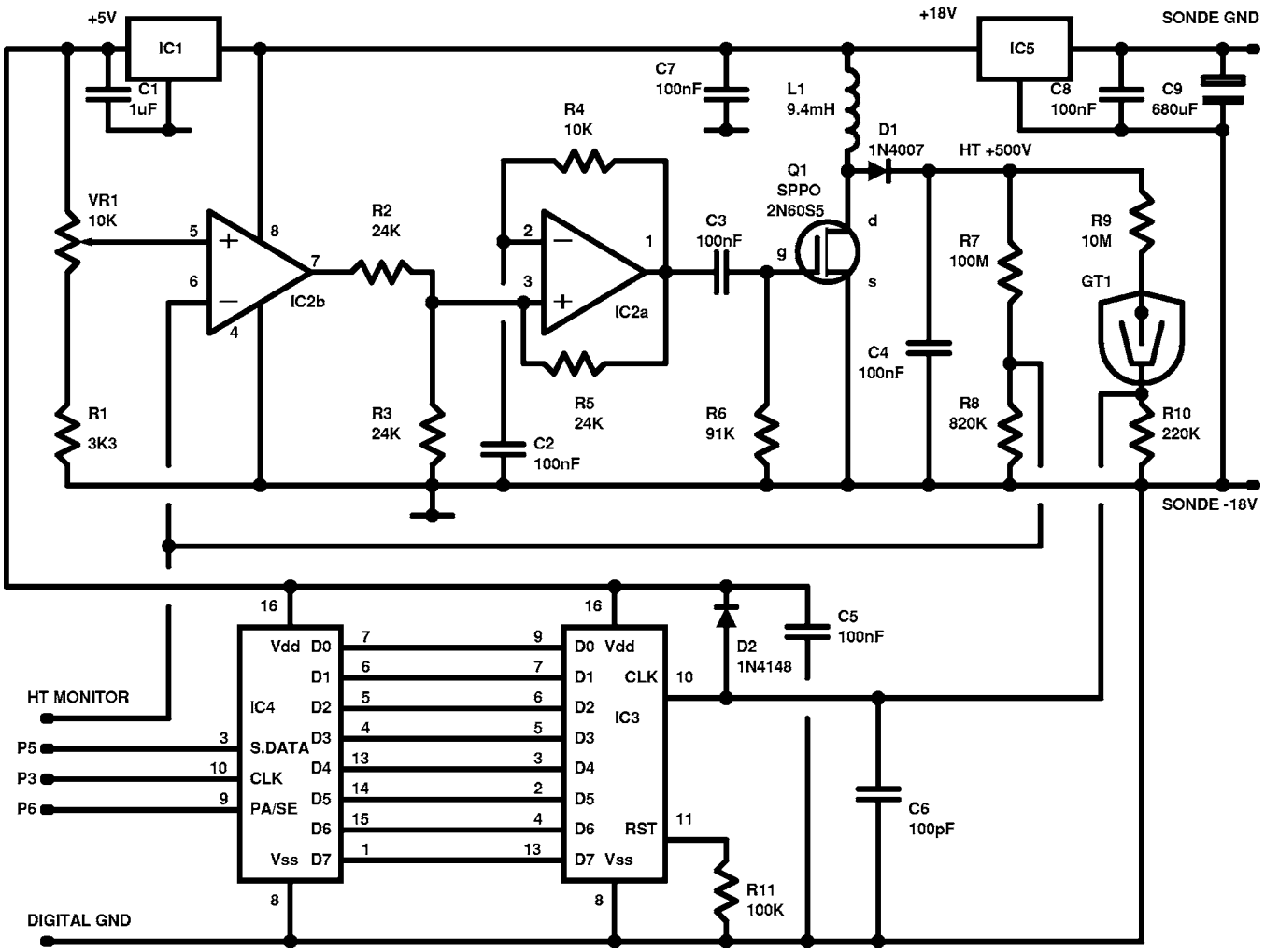

FIG. 1. Schematic of Geiger tube HT supply and radiosonde interface. (Components: all resistors ±2% 50 ppm/°C, except R7, which is ±1% 100 ppm/°C; L1 constructed from two series-connected 4.7 mH miniature axial RF chokes; IC1 MIC2950-6BZ; IC2 TL064; IC3 4040BE; IC4 4014BE; IC5 78L18; GT1 LND714 Geiger tube.) Note that the RS80 radiosonde uses a positive ground.

diosonde UHF radio transmitter. A +5 V subregulated supply is provided by IC1, both as a reference voltage, and to power the digital counter IC3 and shift register IC4. IC4 converts the 8-bit parallel count value on IC3 to serial data. The serial data is transferred using the data acquisition system's microcontroller, programmed to control the digital lines P5 (serial data), P3 (clock), and P6 (select).

The HT voltage can be adjusted using VR1. With a 15 V supply (from which the current consumption is 10 mA), the adjustment range was 30-600 V. Figure 2 shows the measured regulation properties. With VR1 set for a fixed 500 V output, the output varied by less than 0.5 V for input voltages ranging from 15 to 25 V, spanning the typical changes expected from a radiosonde battery in flight.[10] The HT supply was air-wired to the Geiger tube using R9, mounted physically above the circuit board to minimize the possibility of breakdown at low pressure. The system was tested using a pressure chamber to 5 h Pa (~35 km equivalent altitude) with an HT supply of 500 V.

The HT supply and counter were deployed in an atmospheric test ascent in summer conditions, with the equipment mounted on the side of a radiosonde and protected by thin polythene. Two +5 V full scale deflection (FSD) analog channels of the data acquisition system were used to monitor

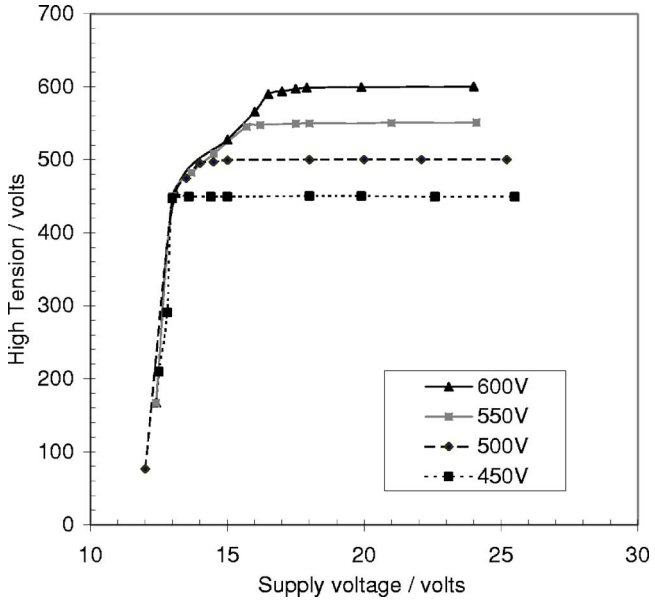

FIG. 2. Sensitivity of the regulated Geiger tube high tension (HT) bias to supply voltage changes for four settings of the HT bias: 450 V, 500 V, 550 V, and 600 V.

(1) the HT voltage at R7-R8, and (2) the battery supply using a 10k:1k 50 ppm/°C potential divider. The microcontroller was programmed to read the analog voltage channels 32 times, and then read the digital counter. Data telemetered over the UHF radio link was time-stamped using the receiving PC's clock, from which the interval between successive readings of the digital counter was found to be 22.1 s.

Some processing was necessary to determine the radiosonde height, the atmospheric properties, and the average count rate. First, the asynchronous meteorological data were interpolated to give values of temperature, pressure, and humidity simultaneous with the analog channels and counter readings. Second, the height of the radiosonde after j successive measurements was computed by summation of the thickness of all j atmospheric layers between the surface and z,

$$z = \sum_{i=1}^{j} \frac{P_i - P_{i-1}}{\bar{\rho} g}, \tag{2}$$

where P_i is the pressure at the ith measurement level, $\bar{\rho}$ is the mean air density in the layer between measurements $(i-1)$ and i, and g is the acceleration due to gravity. ρ was found from the gas law as

$$\rho = \frac{\bar{P}}{R_d(\bar{T} + 273.15)}, \tag{3}$$

where $\bar{P}$ is the mean air pressure (Pa), found from $\frac{1}{2}(P_i + P_{i-1})$, $\bar{T}$ is the air temperature (°C), found from $\frac{1}{2}(T_i + T_{i-1})$, and R_d is the gas constant for dry air (287 J kg^{-1} °C^{-1}). Third, the dew point temperature was found. The dew point T_{dew} is defined by

$$e_s(T_{\mathrm{dew}}) = \bar{e}, \tag{4}$$

where $\bar{e}$ is the water vapor pressure and e_s the saturation vapor pressure. e_s was calculated from temperature T using an exponential parametrization of the form

$$e_s(T) = A \exp\left(\frac{BT}{T + C}\right), \tag{5}$$

with[11] $A = 6.112$ h Pa, $B = 17.67$, and $C = 243.5$ °C. Solving (3) and (4) for T_{dew} gives

$$T_{\mathrm{dew}} = \frac{CK}{(B - K)}, \tag{6}$$

where $K = \ln[\bar{U}\exp\{B\bar{T}/(\bar{T}+C)\}]$ for $\bar{U}$ the mean measured relative humidity.

Figure 3 summarizes results obtained during the test ascent. Figure 3(a) shows that, during the flight, the battery voltage rose to a maximum of 19.6 V, falling to 17.3 V at the burst height of 18.0 km. The HT supply voltage had an average voltage of 556 V, with a standard deviation of 1.2 V. Figure 3(b) shows the changes in T and T_{dew}: the increasing difference between them indicates increasingly dry air. Despite the 13.3% change in the supply voltage, and the change from $T = 24.9$ °C at launch to $T = -52.9$ °C at burst, the change in measured HT voltage was 0.7%. Part of this change can be attributed to thermal drift in the data acquisition system [uncertainty 0.25% (Ref. 10)], or the R7:R8 potential divider (R7 100 ppm/°C, R8 50 ppm/°C).

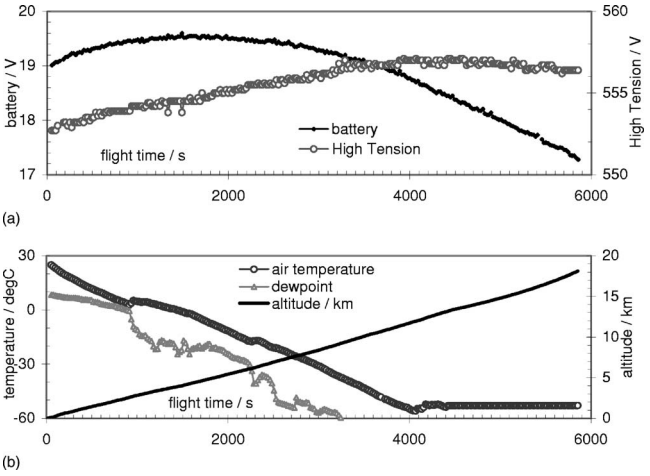

FIG. 3. (a) Telemetered measurements of battery voltage and high tension supply voltage during the atmospheric test flight, as a time series from launch. (b) Simultaneous air temperature, dewpoint temperature, and altitude.

Assuming a potential divider drift of 50 ppm/°C, a 100 °C temperature change would cause a 0.5% uncertainty in the HT measurement. This illustrates that the HT voltage change is sufficiently small to be close to the limitations of the measurement, and within the design constraint of 1%.

Figure 4(a) shows the count rate obtained from successive digital counter readings, as an atmospheric profile. It shows low count rates close to the surface, and an increase with height as the Pfötzner maximum in cosmic rays in the

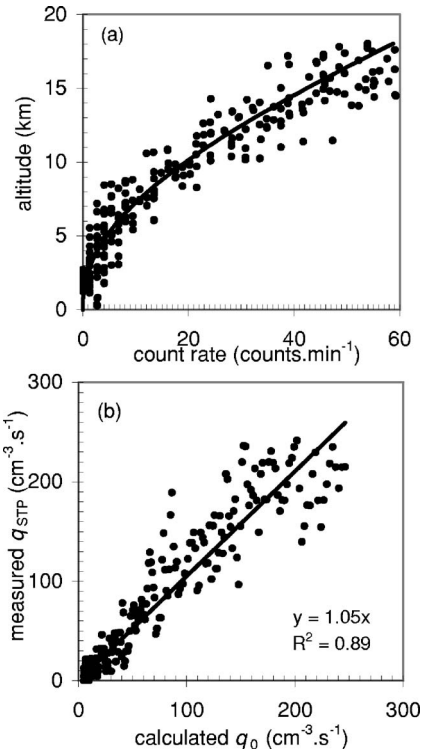

FIG. 4. (a) Vertical profile of count rate obtained during balloon ascent. The fitted line relating counts per minute (CPM) to height was $R' = 8.527 \times 10^{-9}\, z^{2.379} \exp(-3.671 \times 10^{-5}\, z)$, for z in meters. (b) Measured count rates converted to equivalent ion production rate q (at STP: 0 °C, 1013 h Pa) using Eq. (1) with a correction for sensitivity change with temperature, plotted against the calculated ion production rate q_0 at the same altitude.

stratosphere is approached. Using Eq. (1), and the sensitivity of the LND714 tube ($S=66.7$ μRoentgens h^{-1}), the ion production rate was calculated. As a compensation for the small reduction in Geiger tube sensitivity with temperature,[12] the raw count rate was multiplied by T_0/T, where $T_0=273$ K and T the measured air temperature. Figure 4(b) compares the ion production rate measured and that calculated for the same heights at geomagnetic latitude 50°N, using the parametrization[13] summarized in the Appendix. No correction has been applied to the parametrization for geomagnetic or solar changes, but a linear model indicates agreement to 5% in the density-corrected ion production rate.

S. R. Tames fabricated the circuit board, and A. G. Lomas and R. Quillin supervised the balloon launch. D. B. Stephenson obtained the nonlinear fit in Fig. 4(a).

APPENDIX: ION PRODUCTION RATE PROFILE

The vertical profile of ion production rate, $q(z)$, is calculated from the sum of surface ion production rate Q_0 and cosmic ray ion production rate $q_c(z)$ as

$$q(z) = Q_0 \exp\left(-\frac{z}{z_{\mathrm{SI}}}\right) + q_c(z). \tag{A1}$$

The surface ion production rate Q_0 falls off with height z with an exponential scale height z_{SI} ($z_{\mathrm{SI}}=1$ km). Depending on the value of z, $q_c(z)$ is found from

$$z < z_a: \quad q_c(z) = Q_a \exp\left(\frac{z - z_a}{s_a}\right), \tag{A2}$$

$$z_a \leqslant z < z_{\max}: \quad q_c(z) = Q_{\max} \exp\left[-\left(\frac{z - z_{\max}}{s_b}\right)^2\right], \tag{A3}$$

$$z_{\max} \leqslant z \leqslant 30 \text{ km}: \quad q_c(z) = Q_{\max}\left(\frac{z}{z_{\max}}\right) \times \exp\left[-\frac{1}{2}\left(\frac{z}{z_{\max}}\right)^2 + \frac{1}{2}\right]. \tag{A4}$$

In Eqs. (A2)–(A4), Q_a is the cosmic ray ion production rate at a fixed reference height z_a, and $Q_{\max}$ is the maximum cosmic ray ion production rate at $z_{\max}$. The quantities $z_{\max}$, Q_0, Q_a, $Q_{\max}$, and scale heights s_a and s_b are functions of geomagnetic latitude,[6] parametrized[13] as

$$Q_0 = 1.5 + 0.533 \cos^4 \theta,$$

$$Q_a = 15.0 + 17.778 \cos^4 \theta,$$

$$Q_{\max} = 93.5 + 730.0 \cos^4 \theta,$$

$$z_{\max} = 16 + 24.889 \cos^4 \theta,$$

$$z_a = 6.0,$$

$$s_a = -z_a / \ln\left(\frac{Q_0}{Q_a}\right),$$

$$s_b = (z_{\max} - z_a) / \sqrt{-\ln\left(\frac{Q_a}{Q_{\max}}\right)},$$

where θ is the colatitude ($\theta=90-\phi$, for ϕ the geomagnetic latitude). The units of Q_0, Q_a, and $Q_{\max}$ are ion pairs cm^{-3} s^{-1}, and z and s are in km. For $\theta \leqslant 30°$, θ is fixed at 30°, and for $\theta \geqslant 150°$, θ is fixed at 150°.

[1] R. G. Harrison and K. S. Carslaw, Rev. Geophys. **41**, 1012 (2003).
[2] B. A Tinsley, R. P. Rohrbaugh, M. Hei, and K. V. Beard, J. Atmos. Sci. **57**, 2118 (2000).
[3] S. N. Tripathi and R. G. Harrison, Atmos. Res. **62**, 57 (2002).
[4] C. F. Clement and R. G. Harrison, J. Aerosol Sci. **23**, 481 (1992).
[5] K. S. Carslaw, R. G. Harrison, and J. Kirkby, Science **298**, 1732 (2002).
[6] H. V. Neher, J. Geophys. Res. **76**, 1637 (1971).
[7] H. V. Neher and W. H. Pickering, Rev. Sci. Instrum. **13**, 143 (1942).
[8] G. A. Bazilevskaya, M. B. Krainev, and V. S. Makhmutov, J. Atmos. Sol.-Terr. Phys. **62**, 1577 (2000).
[9] http://www.lndinc.com/gm/gamma/714.htm
[10] R. G. Harrison, Rev. Sci. Instrum. **76**, 026103 (2005).
[11] D. Bolton, Mon. Weather Rev. **108**, 1046 (1980).
[12] N. H. Langton and P. P. Brown, J. Sci. Instrum. **39**, 136 (1962).
[13] M. Makino and T. Ogawa, J. Geophys. Res. **90**, 5961 (1985).